Protein Science (2000), *9*:1589–1593. Cambridge University Press. Printed in the USA.

FOR THE RECORD

A simple method for the determination of individual rate constants for substrate hydrolysis by serine proteases

YOUHNA M. AYALA AND ENRICO DI CERA

Department of Biochemistry and Molecular Biophysics, Washington University School of Medicine, Box 8231, St. Louis, Missouri 63110

(RECEIVED February 25, 2000; FINAL REVISION May 6, 2000; ACCEPTED May 10, 2000)

Abstract: A simple method is presented for the determination of individual rate constants for substrate hydrolysis by serine proteases and other enzymes with similar catalytic mechanism. The method does not require solvent perturbation like viscosity changes, or solvent isotope effects, that often compromise nonspecifically the activity of substrate and enzyme. The rates of substrate diffusion into the active site (k_1), substrate dissociation (k_{-1}), acylation (k_2), and deacylation (k_3) in the accepted mechanism of substrate hydrolysis by serine proteases are derived from the temperature dependence of the Michaelis–Menten parameters k_{cat}/K_m and k_{cat}. The method also yields the activation energies for these molecular events. Application to wild-type and mutant thrombins reveals how the various steps of the catalytic mechanism are affected by Na^+ binding and site-directed mutations of the important residues Y225 in the Na^+ binding environment and L99 in the S2 specificity site. Extension of this method to other proteases should enable the derivation of detailed information on the kinetic and energetic determinants of protease function.

Keywords: rate constants; serine proteases; substrate hydrolysis

Serine proteases are involved in several biological functions of physiologic importance, including digestive and degradative processes, blood coagulation, fibrinolysis, complement activation, humoral immunity, and embryonic development (Lesk & Fordham, 1996). Their catalytic mechanism is well understood, although questions remain as to the precise role of D102 in the catalytic triad (Warshel et al., 1989). The mechanism starts with the binding of substrate *S* into the active site of the enzyme *E*, with a second-order rate constant k_1. After formation of the enzyme–substrate complex *ES*, the substrate can either dissociate back into the solution with a rate constant k_{-1}, or become acylated to the active site S195 with a rate constant k_2. The portion of substrate distal to the scissile bond P' is released at this stage. The acyl intermediate *EP* is subsequently hydrolyzed with the assistance of a water molecule to release the portion of substrate proximal to the scissile bond P'' with a rate constant k_3. The series of events leading to substrate hydrolysis can be depicted as follows:

$$E + S \underset{k_{-1}}{\overset{k_1}{\rightleftarrows}} ES \xrightarrow{k_2} EP + P' \xrightarrow{k_3} E + P''. \quad (1)$$

The acylation step is typically rate determining for amide substrates (Brouwer & Kirsch, 1982).

The Michaelis–Menten parameters $s = k_{cat}/K_m$ and k_{cat} accessible to direct experimental measurements are composite functions of the individual kinetic rates in Scheme 1. Specifically,

$$s = \frac{k_1 k_2}{k_{-1} + k_2} \quad (2)$$

$$k_{cat} = \frac{k_2 k_3}{k_2 + k_3}. \quad (3)$$

The parameters have a similar form, but *s* does not depend on the deacylation rate, whereas k_{cat} does not depend on substrate diffusion into the active site and dissociation.

Because four independent rate constants define two independent Michaelis–Menten parameters, knowledge of *s* and k_{cat} from experimental measurements is not sufficient to completely resolve the various steps of the kinetic mechanism in Scheme 1. Methods currently available to obtain the individual rate constants are based on solvent perturbation where the viscosity of the solution is changed with a cosolvent (Brouwer & Kirsch, 1982; Kurz et al., 1987; Stone et al., 1991; Wells & Di Cera, 1992). Alternatively, the solvent isotope effect of water has been used (Cleland, 1995). In these methods, the individual rate constants defining the kinetic mechanism are perturbed to different extent, based on their dependence on diffusion, or the water-mediated hydrolysis. These methods require control experiments to verify that changes in solution conditions do not alter the properties of the enzyme or substrate in

Reprint requests to: Enrico Di Cera, Department of Biochemistry and Molecular Biophysics, Washington University School of Medicine, Box 8231, St. Louis, Missouri; e-mail: enrico@caesar.wustl.edu.

Abbreviations: Ch, choline; FPR, H-D-Phe-Pro-Arg-*p*-nitroanilide; PEG, poly(ethylene glycol); *p*-NA, para-nitroaniline; tPA, tissue plasminogen activator; Tris, tris(hydroxymethyl)aminomethane.

a nonspecific manner (Brouwer & Kirsch, 1982; Kurz et al., 1987; Stone et al., 1991; Wells & Di Cera, 1992). For example, the use of glycerol to change the viscosity of the buffer can change the dielectric properties of the solution, thereby affecting the electrostatic properties of the enzyme in a way that can alter its ability to interact with substrate (Kurz et al., 1987). The use of sucrose as an alternative to glycerol may affect the solubility of enzyme and substrate. Finally, many viscogenic agents also change the extinction coefficient of *p*-NA used to characterize the kinetics of substrate hydrolysis (Wells & Di Cera, 1992), and this effect should be properly taken into account when evaluating k_{cat} values. Here we introduce a simple method to determine the individual rate constants in the kinetic mechanism 1 that has the virtue of not perturbing the solvent with additional solutes.

Results and discussion The method exploits the temperature dependence of s and k_{cat} in Equations 2 and 3. Laidler and Peterman (1979) have used temperature studies of kinetic parameters to resolve some of the individual rate constants in the kinetic mechanism of hydrolases. The temperature dependence of a rate constant obeys the Arrhenius law:

$$k = k_0 \exp\left\{-\frac{E}{R}\left(\frac{1}{T}-\frac{1}{T_0}\right)\right\} \tag{4}$$

where E is the activation energy associated with the rate constant k, R the gas constant, T the absolute temperature, and k_0 the value of k at the reference temperature $T_0 = 298.15$ K. Substitution into Equations 2 and 3 yields

$$s = \frac{k_{1,0}k_{2,0}\exp\left\{-\frac{E_1+E_2}{R}\left(\frac{1}{T}-\frac{1}{T_0}\right)\right\}}{k_{-1,0}\exp\left\{-\frac{E_{-1}}{R}\left(\frac{1}{T}-\frac{1}{T_0}\right)\right\}+k_{2,0}\exp\left\{-\frac{E_2}{R}\left(\frac{1}{T}-\frac{1}{T_0}\right)\right\}} \tag{5}$$

$$k_{cat} = \frac{k_{2,0}k_{3,0}\exp\left\{-\frac{E_2+E_3}{R}\left(\frac{1}{T}-\frac{1}{T_0}\right)\right\}}{k_{2,0}\exp\left\{-\frac{E_2}{R}\left(\frac{1}{T}-\frac{1}{T_0}\right)\right\}+k_{3,0}\exp\left\{-\frac{E_3}{R}\left(\frac{1}{T}-\frac{1}{T_0}\right)\right\}}. \tag{6}$$

Measurements of s and k_{cat} as a function of temperature can resolve all the parameters involved in Equations 5 and 6.

The specificity constant s is the same as k_1 in the range where $k_2 \gg k_{-1}$, and equals k_1k_2/k_{-1} in the range where $k_{-1} \gg k_2$. In the former limit, the slope in the $\ln s$ vs. $1/T$ plot is $-E_1/R$, whereas in the latter the slope is $(E_{-1} - E_1 - E_2)/R$. Activation energies are positive quantities that differ substantially for processes involving diffusion, conformational transitions, or chemical catalysis. The activation energy associated with substrate dissociation (E_{-1}) is much larger than that associated to substrate binding (E_1) or acylation (E_2), and therefore, the term $(E_{-1} - E_1 - E_2)/R$ is expected to be positive. Processes with low activation energy, like substrate diffusion into the active site or acylation, predominate at low temperature where k_2 becomes much larger than k_{-1} and s becomes equal to k_1. On the other hand, substrate dissociation has a high activation energy and becomes predominant at high temperature where $s \to k_1k_2/k_{-1}$. This gives the plot of $\ln s$ vs. $1/T$ a distinct maximum (see below), because the slope changes from negative at low temperature, where information is gathered on k_1 and E_1, to positive at high temperature, where information is obtained on k_1k_2/k_{-1} and $E_{-1} - E_1 - E_2$.

The plot of $\ln k_{cat}$ vs. $1/T$ shows a curvature if k_2 and k_3 become comparable in the temperature range examined. When $k_3 \gg k_2$ in the temperature range studied, the plot of $\ln k_{cat}$ vs. $1/T$ is linear with a slope $-E_2/R$. This information, together with that derived from the $\ln s$ vs. $1/T$ plot, is sufficient to resolve the kinetic rate constants k_1, k_{-1}, and k_2 at the reference temperature, and the activation energies E_1, E_{-1}, and E_2. If $k_2 \approx k_3$ in the temperature range studied, then a curvature is observed in the plot because E_3 is typically larger than E_2. In this case, there are two limiting linear regimes: one at low temperature where $k_{cat} \approx k_3$ and the plot has a slope $-E_3/R$, and the other at high temperature where $k_{cat} \approx k_2$ and the plot has a slope $-E_2/R$. Also, in this case, the parameters in the kinetic Scheme 1 and the associated activation energies can be resolved accurately.

The temperature dependence of s and k_{cat} for substrate hydrolysis by thrombin is shown in Figure 1. Measurements were carried out under 200 mM NaCl to approximate the properties of the Na^+-bound fast form, or 200 mM ChCl to obtain the properties of the Na^+-free slow form. The properties of the fast form were obtained from the extrapolation $[Na^+] \to \infty$ using those of the wild-type in the presence of 200 mM NaCl and those of the slow form in 200 mM ChCl, according to Equations 17c and 29 of Di Cera et al. (1996). The properties of wild-type thrombin in the

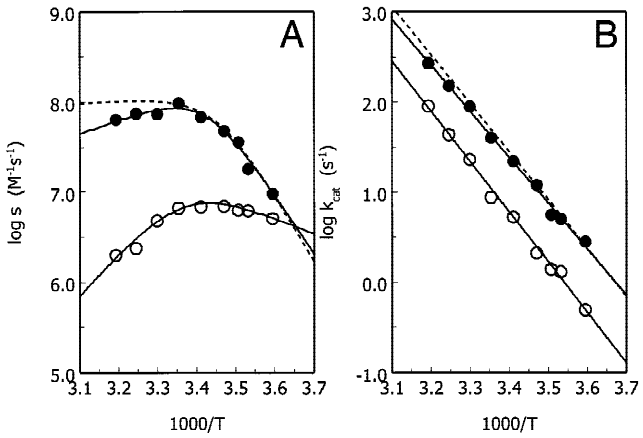

Fig. 1. Arrhenius plots of the specificity constant $s = k_{cat}/K_m$ (**A**) and k_{cat} (**B**) for the cleavage of FPR by thrombin, in the temperature range from 5–45 °C. Note the use of the decimal logarithm in the ordinate. Shown are the values pertaining to wild-type (●) and the slow form (○). The properties of the fast form, shown as a discontinuous line, were obtained from the extrapolation $[Na^+] \to \infty$ using those of the wild-type in the presence of 200 mM NaCl and those of the slow form in 200 mM ChCl, according to Equations 17c and 29 of Di Cera et al. (1996). Experimental conditions are: 5 mM Tris, 0.1% PEG, 200 mM NaCl (wild-type) or 200 mM ChCl (slow form), pH 8.0. Continuous lines were drawn according to Equations 5 and 6 in the text, with best-fit parameter values listed in Table 1. A unique set of best-fit parameters was obtained from a global fit of the s and k_{cat} values. **A:** The curvature in the plot allows for resolution of the four independent parameters in Equation 5 ($k_{1,0}$, $k_{2,0}/k_{-1,0}$, E_1, and $E_{-1} - E_2$). **B:** The linearity of the plot indicates that substrate acylation is rate limiting over the entire temperature range examined, and that k_2 completely defines k_{cat}. This plot yields $k_{2,0}$ and E_2 thereby enabling the derivation of six independent parameters as listed in Table 1.

presence of 200 mM NaCl closely approximate those of the fast form until the temperature is raised above 30 °C. Around the physiological temperature, thrombin behavior is an average of the properties of the slow and fast forms that become equally populated because of the significant drop in Na^+ binding affinity (Guinto & Di Cera, 1996).

Binding of Na^+ to thrombin enhances 46-fold the rate of diffusion of substrate into the active site, presumably through a conformational change that improves accessibility. This result is qualitatively consistent with previous data where the value of k_1 in the two forms was derived from measurements of Michaelis–Menten parameters as a function of viscosity of the solution (Wells & Di Cera, 1992). At low temperature, the value of s decreases more rapidly in the fast form, implying a larger value of E_1 in this form (Table 1). The value of k_1 in the fast form indicates a diffusion-controlled interaction of substrate with the enzyme. Such processes are typically linked to small values of the activation energy. The large value of E_1 in the fast form suggests that additional events must take place to form the enzyme–substrate complex. These events may be related to induced-fit conformational transitions that optimize docking of the substrate into the active site, or more favorable electrostatic coupling between substrate and the Na^+-bound form of the enzyme. In the slow form, the value of E_1 poses a modest energetic barrier to substrate binding, but the rate of diffusion into the active site is considerably smaller than that of the fast form. This suggests that when the substrate finds its way into the active site, the enzyme reacts with little conformational change. As for the rate of substrate binding, the rate of substrate dissociation back into the solution is also more pronounced (22-fold) in the fast form, but occurs with comparable activation energies in the two forms. Binding of Na^+ also enhances the acylation rate that is a direct measure of the k_{cat} of the enzyme in view of the linearity of the Arrhenius plot of $\ln k_{cat}$ vs. $1/T$ (Fig. 1). The enhancement is significant, and the activation energy is similar in the two forms.

Elucidation of the individual rate constants is crucial to understand the properties of alternative conformational states of allosteric proteases like thrombin and also identifies mechanisms that compromise catalytic activity following site-directed mutagenesis. Recent studies have revealed an important role for residue 225 in determining Na^+ binding, allostery and catalytic activity in thrombin and serine proteases (Dang & Di Cera, 1996; Dang et al., 1997; Guinto et al., 1999). The Y225P mutant of thrombin is devoid of Na^+ binding and has reduced catalytic activity relative to the wild-type. Dissection of the individual kinetic rates reveals a compromised substrate binding in the Y225P mutant, with the rate of diffusion into the active site dropping 90-fold relative to the wild-type. The activation energy E_1 is considerably smaller in the mutant and approximates that of the slow form. A significant drop is also seen in the rate of substrate dissociation, whereas the drop in k_2 is less pronounced. The activation energies of these processes are not affected by the mutation. Overall, the behavior of the Y225P mutant approximates that of the slow form, consistent with a loss of Na^+ binding. However, the mutation introduces new features in the molecule that are not necessarily present in the slow form. The crystal structure of the Y225P mutant indicates that the depth of the primary specificity pocket S1 is greatly reduced because of the rearrangement of the carbonyl O atom of K224 due to the presence of P225 (Guinto et al., 1999). This carbonyl O atom occludes the Na^+ channel in the middle, cutting off the environment of the side chain of D189 in the S1 pocket from the water molecules occupying the channel below it. This architecture of the S1 site is shared by all nonallosteric proteases like trypsin, chymotrypsin, and tPA that carry P225 (Guinto et al., 1999). The results in Figure 2 indicate that the movement of the carbonyl O atom of residue K224 causes a drastic loss of the rate of diffusion into the active site. The drop may be due to mechanical factors. Water molecules need to be displaced from the active site for the enzyme–substrate complex to be formed. In the wild-type, water molecules displaced by the incoming substrate may leave the active site using a second aperture at the bottom of the molecule (Guinto et al., 1999), so that the entry point of the substrate and the exit point of the water molecules are different. In the Y225P mutant, the Na^+ channel is closed in the middle and water molecules displaced from the S1 site must leave the active site using the same point of entry as the substrate. This can clearly slow down the rate of productive complex formation because the substrate must wait for water molecules to leave the S1 cavity before making contacts with D189. The enhanced diffusion of substrate into the active site in the wild-type compared to the Y225P mutant shows that the Pro → Tyr conversion occurring during evolution at residue 225 in allosteric serine proteases (Dang & Di Cera, 1996) had the advantage of promoting the productive encounter between substrate and enzyme.

The thrombin mutant L99Y was engineered to test the role of steric hindrance in the S2 site. Several serine proteases, like coagulation factors IXa, Xa, XIIa, plasma kallikrein, tPA, and complement factors C1r, B, C2, and I carry a bulky Tyr at position 99. In coagulation factor IXa, Y99 is in a conformation that blocks access to the S2 site and accounts for the extremely low activity of this enzyme (Hopfner et al., 1999). A similar role has been hypothesized for Y99 in tPA based on the crystal structure (Lamba et al., 1996). The expectation with the L99Y mutant of thrombin was that substrate diffusion into the active site would be compromised. Recent mutagenesis studies have shown that the L99Y mutant has a sevenfold reduction in the k_{cat}/K_m toward synthetic substrates carrying Pro at P2 (Rezaie, 1998) and a fivefold reduc-

Table 1. *Kinetic rate constants and activation energies for FPR hydrolysis by wild-type and mutant thrombins*

	$k_{1,0}$ (μM^{-1} s^{-1})	$k_{-1,0}$ (s^{-1})	$k_{2,0}$ (s^{-1})	E_1 (kcal/mol)	E_{-1} (kcal/mol)	E_2 (kcal/mol)
Fast form	650 ± 50	290 ± 20	50 ± 3	34 ± 3	59 ± 5	24 ± 1
Slow form	14 ± 1	13 ± 1	11 ± 1	8 ± 1	55 ± 5	25 ± 2
wt	390 ± 40	150 ± 10	42 ± 2	31 ± 3	61 ± 3	23 ± 1
Y225P	4.7 ± 0.4	5.0 ± 0.5	32 ± 2	5.5 ± 0.4	48 ± 5	21 ± 1
L99Y	4.0 ± 0.2	100 ± 10	120 ± 10	10 ± 1	32 ± 4	10 ± 1

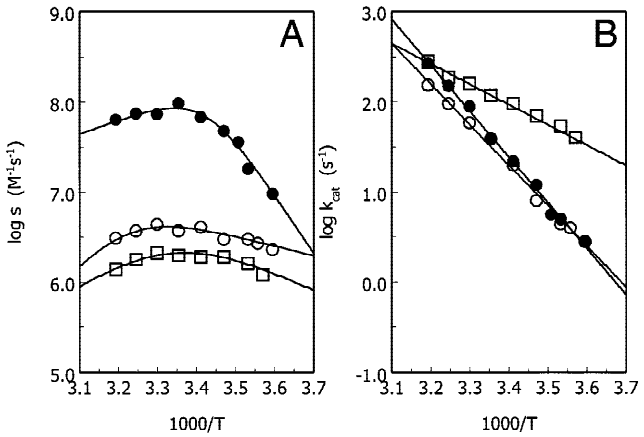

Fig. 2. Arrhenius plots of the specificity constant $s = k_{cat}/K_m$ (**A**) and k_{cat} (**B**) for the cleavage of FPR by wild-type and mutant thrombins, in the temperature range from 5–45 °C. Note the use of the decimal logarithm in the ordinate. Shown are the values pertaining to wild-type (●), and the mutants Y225P (○) and L99Y (□). Experimental conditions are: 5 mM Tris, 0.1% PEG, 200 mM NaCl, pH 8.0. Continuous lines were drawn according to Equations 5 and 6 in the text, with best-fit parameter values listed in Table 1. A unique set of best-fit parameters was obtained from a global fit of the *s* and k_{cat} values, as for the data shown in Figure 1.

tion in the k_{on} for the inhibition of thrombin by antithrombin III (Rezaie, 1997). The data in Figure 2 confirm the expectation of steric hindrance produced by Tyr at position 99. The k_1 is 100-fold lower compared to the wild-type, and the activation energy associated with substrate binding is significantly smaller and comparable to that of the slow form (Table 1), although the mutant binds Na^+. These signatures are reminiscent of those seen in the Y225P mutant, but the rate of substrate dissociation in the L99Y mutant is comparable to that of the wild-type. The side chain of Y99, once displaced to make room for the incoming substrate, causes no steric hindrance to substrate dissociation. The activation energy for substrate dissociation is significantly smaller than that of the wild-type, indicating that the enzyme–substrate complex is energetically more prone to dissociate into the parent species. Finally, the L99Y mutant shows a surprising increase in k_{cat} due to an increased rate of acylation compared to the wild-type. The value of k_2 exceeds that of the fast form, and the activation energy E_2 is significantly lower than that of the wild-type. The enzyme–substrate complex in the L99Y mutant is energetically more prone to undergo acylation, presumably through more favorable contacts made in the transition state that facilitate substrate conversion. Hence, the side chain of Tyr at position 99 opposes substrate diffusion into the active site, but once the enzyme–complex is formed, it actually facilitates substrate conversion.

The information gathered from the temperature dependence of the Michaelis–Menten parameters *s* and k_{cat} is consistent with previous data derived from solvent perturbation techniques (Wells & Di Cera, 1992), and provides additional insights into the energetic signatures of substrate recognition and hydrolysis by thrombin. The advantages of this method are the lack of perturbation of the solvent that may generate nonspecific effects on enzyme and substrate, and the additional information on the activation energies of the various kinetic steps in the mechanism. The method is also valuable when the value of K_m is too large to measure, and k_{cat} cannot be estimated with confidence, as seen with poor substrates or mutant enzymes severely compromised in their catalytic function. In this case, the value of *s* can still be measured accurately, and its temperature dependence provides information on k_1, E_1, the ratio k_2/k_{-1} also known as the stickiness of the substrate (Cleland, 1977), and the difference $E_{-1} - E_2$. We believe that the method presented here will facilitate the dissection of the kinetic rate constants for enzyme mechanisms such as those that involve the large family of serine proteases and many other enzymes.

Materials and methods: Recombinant thrombin and the thrombin mutants L99Y and Y225P were constructed, expressed, purified to homogeneity, and titrated as described (Guinto et al., 1999). Measurements were carried out under experimental conditions of 5 mM Tris, 200 M NaCl, 0.1% PEG, pH 8.0, over the temperature range from 5–45 °C. The pH was precisely adjusted at room temperature to obtain the value of 8.0 at the desired temperature. Tris buffer has a $pK_a = 8.06$ at 25 °C, and a temperature coefficient of $\Delta pK_a/\Delta T = -0.027$ (Stoll & Blanchard, 1990). These properties ensured buffering over the entire temperature range examined. All thrombin constructs were stable over the temperature range studied. The slow form of thrombin was studied by replacing 200 mM NaCl with 200 mM ChCl in the buffer. The chromogenic substrate FPR was synthesized and purified to homogeneity. Progress curves of the release of *p*-NA following the hydrolysis of chromogenic substrate were measured as a function of substrate concentration and analyzed to extract the values of *s* and k_{cat}, after proper correction for product inhibition. The product *p*-NA corresponds to P' in Scheme 1, and its release precedes the deacylation step. The k_{cat} measured from *p*-NA release depends on k_2 and k_3, because the steady state assumption requires *E* to be regenerated. The linearity of the log k_{cat} plot in Figures 1 and 2 shows that acylation is rate limiting in the cases examined. The values of *s* and k_{cat} at different temperatures were simultaneously analyzed in terms of Equations 5 and 6 to extract the individual rate constants and associated activation energies. Proper conversion of decimal to natural logarithm values was applied.

Acknowledgments: This work was supported in part by NIH Research Grants HL49413 and HL58141.

References

Brouwer AC, Kirsch JF. 1982. Investigation of diffusion-limited rates of chymotrypsin reactions by viscosity variation. *Biochemistry 21*:1302–1307.

Cleland WW. 1977. Determining the chemical mechanisms of enzyme-catalyzed reactions by kinetic studies. *Adv Enzymol Related Areas Mol Biol 45*:273–387.

Cleland WW. 1995. Isotope effects: Determination of enzyme transition state structure. *Methods Enzymol 249*:341–373.

Dang QD, Di Cera E. 1996. Residue 225 determines the Na^+-induced allosteric regulation of catalytic activity in serine proteases. *Proc Natl Acad Sci USA 93*:10653–10656.

Dang QD, Guinto ER, Di Cera E. 1997. Rational engineering of activity and specificity in a serine protease. *Nat Biotechnol 15*:146–149.

Di Cera E, Hopfner KP, Dang QD. 1996. Theory of allosteric effects in serine proteases. *Biophys J 70*:174–181.

Guinto ER, Caccia S, Rose T, Fütterer K, Waksman G, Di Cera E. 1999. Unexpected crucial role of residue 225 in serine proteases. *Proc Natl Acad Sci USA 96*:1852–1857.

Guinto ER, Di Cera E. 1996. Large heat capacity change in a protein–monovalent cation interaction. *Biochemistry 35*:8800–8804.

Hopfner KP, Lang A, Karcher A, Sichler K, Kopetzki E, Brandstetter H, Huber R, Bode W, Engh RA. 1999. Coagulation factor IXa: The relaxed conformation of Tyr99 blocks substrate binding. *Struct Fold Des 7*:989–996.

Kurz LC, Weitkamp E, Frieden C. 1987. Adenosine deaminase: Viscosity stud-

ies and the mechanism of binding of substrate and of ground- and transition-state analogue inhibitors. *Biochemistry 26*:3027–3032.
Laidler KJ, Peterman BF. 1979. Temperature effects in enzyme kinetics. *Methods Enzymol 62*:234–257.
Lamba D, Bauer M, Huber R, Fischer S, Rudolph R, Kohnert U, Bode W. 1996. The 2.3 Å crystal structure of the catalytic domain of recombinant two-chain human tissue-type plasminogen activator. *J Mol Biol 258*:117–135.
Lesk AM, Fordham WD. 1996. Conservation and variability in the structures of serine proteinases of the chymotrypsin family. *J Mol Biol 258*:501–537.
Rezaie AR. 1997. Role of Leu99 of thrombin in determining the P2 specificity of serpins. *Biochemistry 36*:7437–7446.
Rezaie AR. 1998. Reactivities of the S2 and S3 subsite residues of thrombin with the native and heparin-induced conformers of antithrombin. *Protein Sci 7*:349–357.
Stoll VS, Blanchard JS. 1990. Buffers: Principles and practice. *Methods Enzymol 182*:24–38.
Stone SR, Betz A, Hofsteenge J. 1991. Mechanistic studies on thrombin catalysis. *Biochemistry 30*:9841–9848.
Warshel A, Naray-Szabo G, Sussman F, Hwang JK. 1989. How do serine proteases really work? *Biochemistry 28*:3629–3637.
Wells CM, Di Cera E. 1992. Thrombin is a Na^+-activated enzyme. *Biochemistry 31*:11721–11730.